Multidielectric response of a two-dimensional electron gas in tilted magnetic fields

Yu. Bychkov,[1,2] C. Faugeras,[1] and G. Martinez[1]
[1]*Grenoble High Magnetic Field Laboratory, MPI-FKF and CNRS, Boîte Postale 166, 38042 Grenoble Cedex 9, France*
[2]*L. D. Landau Institute for Theoretical Physics, Academy of Sciences of Russia, 117940 Moscow V-334, Russia*
(Received 10 March 2004; published 11 August 2004)

The infrared transmission of a multilayer system containing a two-dimensional electron gas is evaluated as a function of magnetic field for a configuration where the multilayer axis is tilted with respect to the direction of the applied magnetic field. The specific case of a doped quantum well is considered and it is shown that under the tilted configuration the cyclotron resonance couples to the mixed plasmon-intersubband mode by pure dielectric effects.

DOI: 10.1103/PhysRevB.70.085306 PACS number(s): 78.30.Fs, 71.38.−k, 78.66.Fd

I. INTRODUCTION

The dielectric constant of a quasitwo-dimensional electronic gas (Q2DEG), in the Faraday configuration, hereafter called the perpendicular Faraday (PF) configuration, has been derived in quantum mechanics in different ways.[1–3] This configuration corresponds to the wave vector $\mathbf{k}$ of the incoming light parallel to the growth z axis of the 2D layer and to the applied magnetic field $\mathbf{B}$. The infrared transmission of a multidielectric layered compound, in the PF configuration, including layer with conducting particles, has been the object of many reports.[4] Results have also been published in the case when, keeping still $\mathbf{k}//\mathbf{B}$, the z axis is rotated by an angle θ with respect to the $\mathbf{k}$ (and $\mathbf{B}$) direction, but without any conducting layer being included in the structure.[5,6] The insertion of a conducting layer in such tilted Faraday (TF) configuration noticeably changes the results because as we shall see in the following, all components of the dielectric tensor $\overleftrightarrow{\varepsilon}$ become nonzero and the structure of the electromagnetic field inside the whole structure is changed. The interpretation of experimental results on Q2DEG for instance, in tilted magnetic fields, is strongly dependant on these aspects and requires an appropriate model. The object of this report is to provide such a model which will be applied to the specific case of a doped quantum well (QW) sandwiched between multilayered dielectric structures of nonconducting materials.

In the first part we will derive the dielectric tensor of the doped QW in the TF configuration and then treat the problem of the multilayer transmission including it. We will give some specific examples based on real experimental results and discuss the consequences in different limits.

II. DIELECTRIC TENSOR OF A CONDUCTING LAYER

Keeping the z direction perpendicular to the plane of the conducting layer of thickness d, the magnetic field $\mathbf{B}$ is applied in a tilted configuration such that $(\mathbf{z},\mathbf{B})=\theta$. The wave vector $\mathbf{k}$ is assumed colinear with the direction of the field but in the opposite direction. The y axis is taken in the incidence plane $(\mathbf{z},\mathbf{k})$. This configuration reflects the experimental configuration encountered in major infrared experiments in high magnetic fields.

If the layer is made of a QW, the electronic states of an electron of charge e and effective mass m^*, are quantized, along the z direction, into electric subbands of energy E_p with corresponding wave functions χ_p ($p=$interger$\geqslant 1$). For each of these electric subbands, the single-particle energy spectrum of electrons, in the x-y direction, in the presence of $\mathbf{B}$, consists of equally spaced $[\hbar\omega_{cz}=\hbar eB_z/(m^*c)]$ energy states known as Landau levels (LL) labeled with an integer index N going from 0 to infinity (B_z being the perpendicular component of the magnetic field). Each LL is furthermore split by spin effects and has a degeneracy $G_B=eB_\perp/h$. For the tilted configuration, the LL attached to a given electric subband interact with some of the LL attached to the upper electric subband in a way which is well documented in the literature.[7] This is a strong interaction which can, in the case of a square QW, be treated only in perturbation theory.[7] As we shall see in the following, the main effects for a tilted configuration originates from this mixing of the z and x-y part of the 2DEG wave function and therefore it is important that this effect be treated with the best accuracy. As demonstrated by Merlin[8] and Maan,[9] this is the case, if we assume the z-confining potential $V(z)$ be parabolic of the form $V(z)=(m^*/2)\Omega^2z^2$: the interelectric subband energy is now constant and equal to $\hbar\Omega$ and the coupling can be evaluated analytically at all orders. Merlin has treated this one-electron model in quantum mechanics and obtains an exact analytical solution of the different eigenvalues and related wave functions. It is, however, not easy from such an approach to derive the dielectric function of the Q2DEG gas.

On the other hand, there exists an alternative to treat the same model using a semiclassical approach, more appropriate to calculate the dielectric tensor: one can solve the same problem using the equation of motion for the position $\mathbf{r}=(x,y,z)$ and the corresponding velocity $\mathbf{v}=d\mathbf{r}/dt$ of the electron subjected to $\mathbf{B}$ and to the electromagnetic field $\mathbf{E}$:

$$m^*\frac{d\mathbf{v}}{dt}=-m^*\gamma\mathbf{v}+\frac{e}{c}(\mathbf{v}\times\mathbf{B})-m^*\Omega^2z\hat{z}+e\mathbf{E}, \qquad (1)$$

where γ is the inverse of the scattering time and $\hat{z}$ the unit vector in the z direction. Taking the time evolution of $\mathbf{E}$ as $e^{-i\omega t}$, Eq. (1) can be written in a matrix form as $\hat{\mathbf{M}}\cdot\mathbf{r}$

$=(e/m^*)\mathbf{E}$ or $\mathbf{r}=(e/m^*)\widehat{\mathbf{M}^{-1}}\cdot\mathbf{E}$. Defining $\tilde{\omega}=\omega+i\gamma$, $\widehat{\mathbf{M}^{-1}}$ has the following components:

$$\widehat{\mathbf{M}^{-1}}=\begin{bmatrix}\alpha_{xx} & \alpha_{xy} & \alpha_{xz}\\ -\alpha_{xy} & \alpha_{yy} & \alpha_{yz}\\ -\alpha_{xz} & \alpha_{yz} & \alpha_{zz}\end{bmatrix}, \tag{2}$$

with

$$\alpha_{xx}=\frac{\tilde{\omega}(\Omega^2-\tilde{\omega}\omega)}{\omega D},$$

$$\alpha_{xy}=i\frac{\omega_{cz}(\Omega^2-\tilde{\omega}\omega)}{\omega D},$$

$$\alpha_{xz}=i\frac{\omega_{cy}\tilde{\omega}}{D},$$

$$\alpha_{yy}=\frac{\tilde{\omega}(\Omega^2-\tilde{\omega}\omega)+\omega\omega_{cy}^2}{\omega D},$$

$$\alpha_{yz}=\frac{\omega_{cy}\omega_{cz}}{D},$$

$$\alpha_{zz}=\frac{\omega_{cz}^2-\tilde{\omega}^2}{D}, \tag{3}$$

with

$$D=\tilde{\omega}^3\omega-\Omega^2\tilde{\omega}^2-\omega_c^2\tilde{\omega}\omega+\omega_{cz}^2\Omega^2 \tag{4}$$

and $\omega_{cz}=eB_z/(m^*c)$, $\omega_{cy}=eB_y/(m^*c)$, $\omega_c^2=\omega_{cz}^2+\omega_{cy}^2$.

For a volumetric carrier density n_V, the polarization $\mathbf{P}=n_Ve\mathbf{r}$ and the components of the electronic part of the tensor $\overleftrightarrow{\varepsilon}$ are given by $\varepsilon_{ij}^{el}=\omega_p^2\alpha_{ij}$ with $\omega_p^2=4\pi n_Ve^2/m^*$ being the effective plasma frequency squared directly related to the strength of the absorption of the cyclotron resonance (CR) transition. In the case of a doped squared QW, of width L, we assume $n_V=n_S/L$ where n_S is the areal electronic density. Adding the high frequency part (ε_∞) to the lattice contribution of the dielectric constant of the polar material hosting the carriers, the components of the total $\overleftrightarrow{\varepsilon}$ can be written as:

$$\varepsilon_{ij}=\varepsilon_\infty\left(1+\frac{\omega_{\mathrm{TO}}^2-\omega_{\mathrm{LO}}^2}{\tilde{\omega}^2-\omega_{\mathrm{TO}}^2}\right)\delta_{ij}+\omega_p^2\alpha_{ij}, \tag{5}$$

where ω_{TO} and ω_{LO} are the transverse and longitudinal optical frequencies of the infrared active phonon, respectively. The lattice part of $\overleftrightarrow{\varepsilon}$ is written here for a cubic crystal but can be easily extended to a tetragonal one, this contribution to $\overleftrightarrow{\varepsilon}$ remaining diagonal. Note that for $\theta=0$ (PF configuration for which $\omega_{cz}=\omega_c$) the components α_{ij} reduce to the standard results

$$\alpha_{xx}^{\mathrm{PF}}=-\frac{\tilde{\omega}}{\omega(\tilde{\omega}^2-\omega_c^2)},$$

$$\alpha_{xy}^{\mathrm{PF}}=-i\frac{\omega_{cz}}{\omega(\tilde{\omega}^2-\omega_c^2)},$$

$$\alpha_{yy}^{\mathrm{PF}}=\alpha_{xx}^{\mathrm{PF}},$$

$$\alpha_{zz}^{\mathrm{PF}}=-\frac{1}{\omega\tilde{\omega}-\Omega^2}$$

$$\alpha_{xz}^{\mathrm{PF}}=\alpha_{yz}^{\mathrm{PF}}=0, \tag{6}$$

The poles of the general dielectric constant are ω_{TO} and the two zeros of D [Eq. (4)] which have a positive real part. Neglecting the damping, these two poles are given by

$$\omega_{1,2}^2=\frac{\Omega^2+\omega_c^2}{2}\pm\frac{[(\Omega^2-\omega_c^2)^2+4\Omega^2\omega_{cy}^2]^{1/2}}{2}. \tag{7}$$

We note that these solutions are exactly the same than those obtained from the quantum mechanical treatment of the problem.[8,9] In the PF configuration they correspond to the pure CR mode ω_c and the interelectric-subband mode Ω. This last mode is not active in the PF configuration since the component E_z of $\mathbf{E}$ is zero in this case. In the TF configuration, however, it becomes active and the pole corresponding to ω_c is also changed in a way which is not negligible. For very large values of Ω, (two-dimensional limit), this pole tends to ω_{cz} but this is only true in this limit.

Before analyzing the way to derive the multidielectric response of conducting systems with such a dielectric constant, it is worth to comment on the approximations involved in the present model. It is clear that this model, derived in the limit $k\rightarrow 0$, ignores retardation effects as well as all electron-electron interactions. However, due to the Kohn theorem, these interactions should not influence, *a priori*, the cyclotron resonance response. This is true as long as nonparabolicity (NP) effects are neglected. In the same idea, this semiclassical approach does not include the LL quantization of the electronic levels, which is also not critical when NP effects are neglected. They are, however, not always negligible, especially at high fields, and therefore, in this case, one should adapt the model to take them into account: a way to do so is explained in the Appendix.

A second point to be discussed is the approximation made by treating the square QW as a parabolic one. Note first that in Eq. (1) as well as in the parabolic model,[8,9] the effective mass m^* is the same along all directions: along the z direction its real physical meaning is not always clear especially for QW widths lower than the magnetic field length. In the PF configuration [Eq. (6)], the characteristics of the well enters in $\varepsilon_{ij}^{\mathrm{el}}$ and does not depend on the magnetic field. It can indeed be compared to known results.[1,10] In general the confined character of the Q2DEG is taken into account by the introduction of the so-called form factors appearing as a correction to ω_p^2, replacing the geometrical thickness L by an effective length L_{eff} which is different. This correction applies to all components $\varepsilon_{ij}^{\mathrm{el}}$ in Eq. (5). This is related to the strength of the CR transition and will be further discussed when comparing the predictions of the model to real experimental results. A second correction has also to be applied to $\varepsilon_{zz}^{\mathrm{el}}$ as a multiplicative factor which is the optical oscillator strength of the transition between the electric subbands levels[10] which depends of the shape of the z-confining po-

tential. Restricting the discussion to transitions between the two lower electric subband levels, $(E_1 \rightarrow E_2)$ this quantity is defined as $f_{1,2}=2|\langle\chi_1|p_z|\chi_2\rangle|^2/(m^*\hbar\omega_{2,1})$ (p_z being the z component of the momentum, $\hbar\omega_{2,1}$ the energy splitting of levels E_1 and E_2) and is about 0.96 for an infinite square QW and 1 for the parabolic QW. They therefore do not differ much in that case but the form factor itself could vary and only a comparison with real experimental results could evaluate the approximation made in the present model.

Finally, it is easy with a parabolic model to go to different limits and in particular to the three-dimensional (3D) case, letting $\Omega \rightarrow 0$, while keeping ω_p^2 constant. This 3D case has been extensively studied and following the earlier work of Ginzburg[11] reviewed in more general configurations by Palik and Furdyna.[12] It can be shown that the present results agree with these previous studies.

III. MULTIDIELECTRIC TRANSFER MATRIX

Once the dielectric tensor of the layer is defined, we are in position to evaluate the different electromagnetic modes $\mathbf{q}=\mathbf{k}c/\omega$ that such a medium can sustain: this is obtained in a standard way[13] by solving the following determinant:

$$|q^2\delta_{ij} - q_i q_j - \varepsilon_{ij}| = 0 \tag{8}$$

in which all components q_x are zero by symmetry and q_y is conserved. This equation has four solutions $\mathbf{q}_\lambda$ or $\mathbf{k}_\lambda$ for which $q_\lambda^2 = q_{\lambda,z}^2 + q_y^2$. In the absence of free particles this set of solutions decomposes into two subsets of solutions $\pm\mathbf{q}_{\mathrm{TM}}$ and $\pm\mathbf{q}_{\mathrm{TE}}$ corresponding to the standard transverse magnetic (TM) and transverse electric (TE) modes, respectively[5] The introduction of free particles mixes these two sets of modes and the actual solutions have to be obtained by numerical computation.

In order to evaluate the transmission of a multilayer structure one has to express for each layer the transmitted electromagnetic field as a function of the incident one. The total electric field $\mathbf{E}$ and the corresponding magnetic field $\mathbf{H}$ can be written formally in each medium as a linear combination of the four waves

$$\mathbf{E} = \sum_\lambda a_\lambda \mathbf{E}_\lambda e^{ik_{\lambda,z}z},$$

$$\mathbf{H} = \sum_\lambda a_\lambda \mathbf{q}_\lambda \wedge \mathbf{E}_\lambda e^{ik_{\lambda,z}z}, \tag{9}$$

where a_λ is the amplitude of the mode λ with components of $\mathbf{E}_\lambda$ written as $E_{\lambda,x}, E_{\lambda,y}, E_{\lambda,z}$. Since only two components, for each wave, are independent, one can normalize these components for instance as $X_\lambda = E_{\lambda,x}/E_{\lambda,y}$, 1, $Z_\lambda = E_{\lambda,z}/E_{\lambda,y}$. Finally, it is easier to define a third quantity $Y_\lambda = q_y Z_\lambda - q_\lambda$.

In order to solve for the a_λ coefficients of Eq. (9) one has to write the standard continuity relations for the tangential components of $\mathbf{E}$ and $\mathbf{H}$ which are E_x, H_y, H_x, E_y across the interfaces at $z=0$ and $z=-d$. At each interface, one obtains a system of four linear equations relating $\mathbf{A}$, the vector of components a_λ, either to $\mathbf{F}_i$, a vector of components $E_x(z=0)$, $H_y(z=0)$, $H_x(z=0), E_y(z=0)$ or to $\mathbf{F}_t$ the vectors of components $E_x(z=-d)$, $H_y(z=-d)$, $H_x(z=-d)$, $E_y(z=-d)$. These continuity relations can be expressed in matrix notation as $\mathbf{F}_i = \widehat{\mathbf{M}_0}\cdot\mathbf{A}$ at $z=0$ and similarly at $z=-d$, $\mathbf{F}_t = \widehat{\mathbf{M}_d}\cdot\mathbf{A}$. Then the relations between the incident and transmitted fields are $\mathbf{F}_t = \widehat{\mathbf{M}^t}\cdot\mathbf{F}_i$ where $\widehat{\mathbf{M}^t} = \widehat{\mathbf{M}_d}\cdot\widehat{\mathbf{M}_0^{-1}}$ is the transfer matrix which is specific for each layer m and therefore should be written more explicitly as $\widehat{\mathbf{M}_m^t}$.

When the structure is made of M different layers corresponding to different materials with specific dielectric constant, the total transfer matrix of the structure is[5] $\widehat{\mathbf{M}^T} = \prod_{m=1}^{M}\widehat{\mathbf{M}_m^t}$.

IV. TRANSMISSION OF THE MULTILAYER SYSTEM

We will assume in the following that the multilayer structure is inside the vacuum and label the corresponding electromagnetic parameters with an index 0. In the absence of any polarization, the components of the incident field $\mathbf{F}_{i,0}$ are written as $(E_{x,0}, H_{y,0}, E_{y,0}, H_{x,0})$ and those of the outgoing field $\mathbf{F}_{t,0}$ as $(E_{x,t}, H_{y,t}=q_{z,0}E_{x,t}, E_{y,t}, H_{x,t}=-E_{y,t}/q_{z,0})$. The explicit variation of the incident waves as a function of z is written as

$$E_{x,0} = F\exp(ik_{z,0}z) + G\exp(-ik_{z,0}z),$$

$$H_{y,0} = -q_{z,0}[(F\exp(ik_{z,0}z) - G\exp(-ik_{z,0}z)],$$

$$E_{y,0} = I\exp(ik_{z,0}z) + J\exp(-ik_{z,0}z),$$

$$H_{x,0} = \frac{1}{q_{z,0}}[I\exp(ik_{z,0}z) - J\exp(-ik_{z,0}z)], \tag{10}$$

where G and J refer to the amplitude of incident waves, F and I to that of the reflected ones and $q_{z,0} = -\cos(\theta)$.

Taking the origin $z=0$ at the surface of the sample, $\mathbf{F}_{t,0} = \widehat{\mathbf{M}^T}\cdot\mathbf{F}_{i,0}(z=0)$ which relates the components of the transmitted field to the parameters F, G, I, and J. In a more convenient form, one can define new vectors $\mathbf{E}_T$ of components $(E_{x,t}, E_{x,t}, E_{y,t}, E_{y,t})$ and $\mathbf{V}$ of components (F, G, I, J) such that $\mathbf{E}_T = \widehat{\mathbf{M}}\cdot\mathbf{V}$ with:

$$\widehat{\mathbf{M}} = \widehat{\mathbf{m}_0}\cdot\widehat{\mathbf{M}^T}\cdot\widehat{\mathbf{m}_1},$$

$$\widehat{\mathbf{m}_0} = \begin{bmatrix} 1 & 0 & 0 & 0 \\ 0 & -\cos(\theta)^{-1} & 0 & 0 \\ 0 & 0 & 1 & 0 \\ 0 & 0 & 0 & \cos(\theta) \end{bmatrix},$$

$$\widehat{\mathbf{m}_1} = \begin{bmatrix} 1 & 1 & 0 & 0 \\ \cos(\theta) & -\cos(\theta) & 0 & 0 \\ 0 & 0 & 1 & 1 \\ 0 & 0 & -\cos(\theta)^{-1} & \cos(\theta)^{-1} \end{bmatrix}. \tag{11}$$

This corresponds to a system of four equations which has to be solved for $E_{x,t}/G, E_{y,t}/G, E_{x,t}/J$, and $E_{y,t}/J$. This resolu-

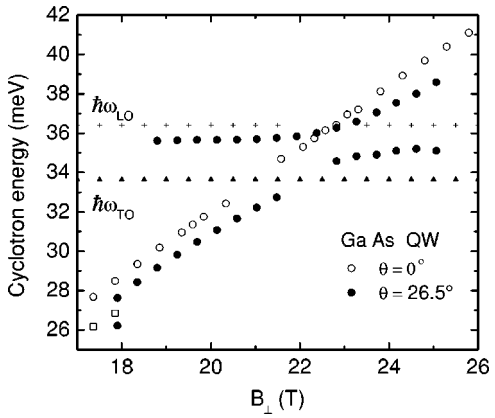

FIG. 1. Energies of the minima of transmission, at 1.8 K, of a two-dimensional electron gas imbedded in a GaAs quantum well, of width 13 nm, around the TO energy of this compound, as a function of the component of the field perpendicular to the QW plane $B_\perp$. These data are obtained in PF configuration (open dots) and in the TF configuration for an angle $\theta=26.5°$ (full dots). Full triangles and crosses are the observed phonon structures corresponding to the TO and LO (slab modes) of the structure, respectively.

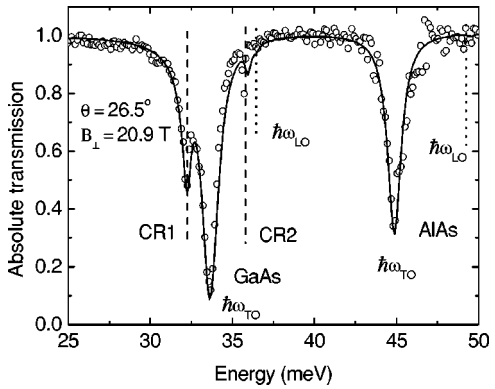

FIG. 2. Absolute transmission spectrum (empty dots), at 1.8 K, of a two-dimensional electron gas imbedded in a GaAs quantum well, of width 13 nm, in a TF configuration with an angle $\theta=26.5°$ and $B_\perp=20.9$ T. The dotted lines refer to the LO energies of GaAs and AlAs and the dashed lines to the two cyclotron like transitions CR1 and CR2 (see text). The continuous line is the fit of the model to the data.

tion can be performed analytically if we consider special polarized conditions for the incoming light. For instance if we assume the incident electric field polarized along the x direction (the so-called TE polarization) F, G, and I are non zero but $J=0$ and $E^{\mathrm{TE}}_{x,t}/G$, $E^{\mathrm{TE}}_{y,t}/G$ can be expressed as function of the matrix elements of $\hat{\mathbf{M}}$. Similarly, if we assume the incident magnetic field polarized along the x direction (the so-called TM polarization), $G=0$ but not I, J, and F, and we can solve the system for $E^{\mathrm{TM}}_{x,t}/J$, $E^{\mathrm{TM}}_{y,t}/J$. This finally allows to find the transmission for any kind of incident polarization.

V. COMPARISON WITH EXPERIMENTAL RESULTS

We now compare the predictions of the model with results which have been recently published.[14] The experimental data correspond to infrared magneto-absorption of a single and symmetrically doped QW of GaAs sandwiched between GaAs-AlAs superlattices, the whole epilayer structure being liftoff from the native GaAs substrate and deposited on a Si substrate.[15] The interest in this case is that the data correspond to *absolute* values of the transmission, for nonpolarized light, performed in PF and TF configurations for which all magnetic field dependent structures can be isolated and compared to the present model. As an example, the experimental energies obtained on such a structure are displayed in Fig. 1, as a function of $B_z=B_\perp$, for a specific sample with a doped GaAs QW of width $L=13$ nm. This QW is sandwiched between two superlattices (period 2.6 nm GaAs/1.3 nm AlAs) of 58 and 12 periods, respectively, the epilayer starting and ending with a GaAs cap layer of 20 nm. For each individual layer the dielectric constant and the corresponding transfer matrix has to be evaluated along the lines described earlier. The doping level of the QW is determined by the adjustment of the CR oscillator strength, in the field range where this resonance splits due to NP effects, assuming the one-electron model for oscillator strength (see the Appendix). In the present case we use, for fitting the data, the value of the concentration $n_S=9\times10^{11}\mathrm{cm}^{-2}$ whereas a value of $n_S^{\mathrm{tr}}=9.4\times10^{11}\mathrm{cm}^{-2}$ is obtained from transport measurements on a parent nonliftoff sample. The reason for this slight discrepancy is not clear at present.

The data which are displayed in Fig. 2 reproduce the absolute transmission spectra obtained at fixed value of the magnetic field. There are features which do not depend on the magnetic field: they correspond to a strong absorption related to the TO phonons of GaAs and AlAs and also weak absorption lines related to the corresponding LO modes (vertical dotted lines) which are known to become active in absorption for thin slabs[5] in the TF configuration. These LO structures are less visible for the tilt angle θ corresponding to Fig. 3 but become important when increasing θ.[14] The magnetic field dependent structures are two additional lines related to the CR and labeled CR1 and CR2 (vertical dashed lines) in the order of increasing energies: at low fields CR1 varies much like the standard CR line observed in the PF configuration and CR2 remains pinned to some energy lower than the LO energy of the GaAs layers. Upon increasing the field there is a clear anticrossing between these transitions, and at high fields CR1 remains pinned (at the same energy than CR2 at low fields within the experimental errors) whereas CR2 evolves like a CR transition. Experimentally it is observed that the anticrossing increases with θ but the pinning energy remains the same for a given sample.[14] For this sample the experimental pinning energy is 35.5 ± 0.05 meV.

The continuous line in Fig. 2 is the fit of the data by adjusting the different parameters which enter the model. The phonon contribution which enters in the diagonal part of $\overleftrightarrow{\varepsilon}$ can be fitted with well known parameters as reported in the literature: we use here, for GaAs, the values of $\hbar\omega_{\mathrm{TO}}=33.6$ meV, a damping parameter $\gamma_{\mathrm{TO}}(\mathrm{GaAs})=0.37$ meV, a static value of the dielectric constant $\varepsilon_0=12.5$ and $\varepsilon_\infty=10.6$. Similarly for AlAs we use $\hbar\omega_{\mathrm{TO}}=45.9$ meV, $\gamma_{\mathrm{TO}}(\mathrm{AlAs})$

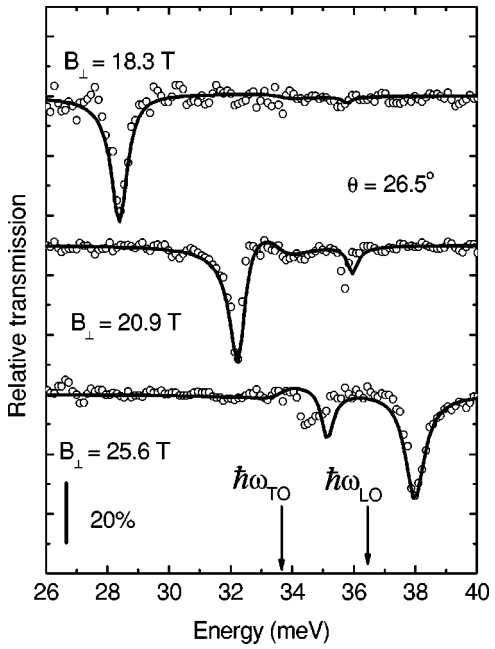

FIG. 3. Fit of the relative transmission curves at $\theta=26.5°$ for different values of $B_\perp$. The curves are shifted for clarity. Empty dots are experimental points and the full continuous curves the corresponding calculated relative transmission spectra.

$=0.56$ meV, $\varepsilon_0=9.9$, and $\varepsilon_\infty=8.16$. These values are kept fixed for all configurations, angles, and magnetic field values. The fit of the features which are magnetic field dependent is more easily done on the experimental spectra of the relative transmission[14] obtained by dividing the absolute transmission spectra, at fixed value of field, by that at 0 T. In these spectra all phonons features disappear as shown in Fig. 3. Though these features do not appear any more, they may be indirectly seen through interferences effects between the TO and the CR absorptions and therefore spectra in which both transitions overlap should be analyzed keeping in mind this potential problem.

The fitting procedure, which gives rise to the continuous spectra displayed in this figure, involves different steps. One has first to evaluate the effective mass m^* entering into the expression of ω_p^2, ω_{cz}, and ω_{cy} and the damping parameter of the electrons this is done by fitting spectra in the PF configuration. It is assumed, since the cyclotron motion depends only on $B_\perp$ that, for a given value of this parameter, m^* should be the same. Therefore, we are left with two parameters to fit the spectra in the TF configuration, the angle θ and the inter-electric subband energy $\hbar\Omega$. θ has also to be fitted because, in the TF configuration, the Si substrate, supporting the epilayer, is glued to a sample holder wedged mechanically by a known angle θ_m. The Si substrate is, however, itself wedged by few degrees to avoid interferences effects, and there is always an uncertainty of few degrees between θ and θ_m.[14] For a given value of θ and knowing the total value of the applied magnetic field, $B_\perp$ is deduced and therefore m^*. The fit of the CR line is now dependent on Ω. Therefore, there is some iterative process between θ and Ω which converges rapidly. Of course, if different experimental data are obtained with different angles, the fitting process has

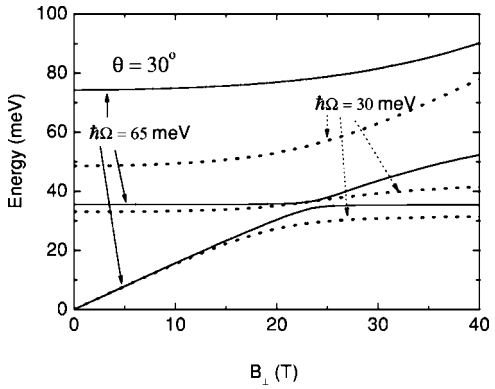

FIG. 4. Variation of the zeros of the component ε_{zz} for a TF configuration with $\theta=30°$ as a function of $B_\perp$. Full lines are related to an intersubband energy $\hbar\Omega=65$ meV and dotted lines to $\hbar\Omega=30$ meV.

to use the same value of Ω,[14] for a given sample. With all these constrains, the fitted spectra displayed in Fig. 4, are obtained for $\hbar\Omega=65$ meV and $\theta=26.5°$. Indeed, when looking at different samples with the same width L (of 13 nm) but different concentrations, one finds for $\hbar\Omega$ values of 63 ± 3 meV whereas for samples with a QW width of 10 nm $\hbar\Omega=105\pm3$ meV.[14] Finally, θ is obtained with an uncertainty of $\pm0.5°$ and therefore $B_\perp$ is given with a corresponding error-bar in the TF configuration.

As can be seen in Fig. 4, the overall agreement is encouraging knowing the simplicity of the model. It can indeed reproduce the anticrossing behavior observed experimentally, including its increase with the angle and validates the experimental finding (Fig. 1) that the CR lines in the TF configuration does not depend only on $B_\perp$ as reported sometimes in the literature. It is also important to stress that, at this level of precision, the model works for different samples with different well widths and carrier concentrations and therefore it has captured the main physics which appears in such studies. As a consequence we are in a position to assign the pinning level which appears in the data below the LO energy.

VI. DISCUSSION OF THE RESULTS

It is clear that the interaction observed in the TF configuration originates from the z components of the dielectric tensor. In particular, the energy of the pinning level, appearing in Fig. 1 for instance, corresponds to one of the zeros of ε_{zz}, the zz component of the total dielectric tensor (Eq. (5)). Neglecting damping, these zeros are solutions of the following equation:

$$\omega^6-(\omega_{\mathrm{LO}}^2+\omega_c^2+\Omega_p^2)\omega^4+[\omega_{\mathrm{LO}}^2\omega_c^2+\Omega^2(\omega_{\mathrm{LO}}^2+\omega_{cz}^2)+\Omega_p^2(\omega_{\mathrm{TO}}^2+\omega_{cz}^2)]\omega^2-\omega_{cz}^2(\Omega^2\omega_{\mathrm{LO}}^2+\Omega_p^2\omega_{\mathrm{TO}}^2)=0, \tag{12}$$

where $\Omega_p^2=\omega_p^2/\varepsilon_\infty$.

For a finite value of the magnetic field, ε_{zz} has three zeros which vary with $B_\perp$ as illustrated in Fig. 4. These results are obtained using as parameters, a tilt angle $\theta=30°$, $\hbar\omega_{\mathrm{TO}}$

$=33.6$ meV and $\hbar\omega_{LO}=36.3$ meV, $n_S/L=6.92\times10^{17}\text{cm}^{-3}$, and a fixed value of the effective mass $m^*=0.072m_0$. These are parameters close to those used to fit the data in Fig. 3. One set of data in Fig. 4 (full lines) is using the value of the intersubband energy $\hbar\Omega=65$ meV (as in Fig. 3) which is higher than $\hbar\omega_{LO}$(GaAs) and the second set of data (dotted lines) corresponds to another value $\hbar\Omega=30$ meV which is lower in energy than $\hbar\omega_{LO}$. In both cases, at low value of the magnetic field, the zero of lower energy corresponds to the "cyclotron-like" transition whereas the two other modes of higher energy have a mixed character of phonon and intersubband excitations. At zero magnetic field these modes are indeed the intersubband-phonon-plasmon modes of quasitwo-dimensional system as first observed by Pinczuk *et al.*[16] The analysis of experimental data[14] shows that the mode just below $\hbar\omega_{LO}$ is indeed the one which interacts with the CR mode (Fig. 1): for instance at $B_\perp=0$ the energy of the calculated mode is 35.5 meV which compares very well with the experimental findings displayed in Fig. 2. The observed anticrossing is a pure dielectric effect which does not imply any specific electron-phonon interaction.

The anticrossing splitting of ε_{zz} is increasing with the angle θ but also when decreasing Ω as evidenced in Fig. 4. One notes that the anticrossing implies also the highest energy hybrid mode and one expects some strongly nonlinear variation of the "3CR-like" mode for samples where the intersubband energy is significantly lower than the energy of the phonons. This prediction has to be confirmed by experiments performed on samples with appropriate characteristics. In any case, the interaction is zero when $\theta=0$ but also disappears when increasing $\hbar\Omega$. This interaction goes indeed to zero in the pure two-dimensional case, for any value of θ. In the 3D case, when $\Omega=0$, Eq. (12) reduces to known results[12,17] which means that for finite values of the magnetic field and one-phonon mode polar material one has always three solutions for the zeros of ε_{zz}. In the absence of magnetic field on the other hand, there are only two solutions which correspond, in the 3D case, to the well known coupled plasmon-phonon modes $\omega^{\pm}$.[12,18] This discussion is qualitative because the real interaction, depicted in Fig. 3, implies all z dependent components of the dielectric tensor.

As clearly seen in Fig. 3, the model presents however some deficiencies: whereas it overestimates the splitting of the CR1-CR2 components at low fields, it underestimates it at high fields. In the same time the component which remains pinned has an oscillator strength smaller than the experimental one at low fields and higher than the experimental one at high fields. Both discrepancies are systematic for different samples and tell that the model may have to be refined. In the present model, the strength of the absorption is only governed by one parameter ω_p^2 [Eq. (6)], a quantity which combines a single value of the effective mass (for $\nu\leqslant2$) and that of the QW width L. This quantity, using the parameters described before, reproduces quite well the strength of the CR absorption in the PF configuration. Therefore, it should not be changed for the in-plane components of the dielectric tensor.

The effective mass parameter, entering Eq. (1), has, however, no clear physical meaning along the z direction. Therefore, one could introduce a parameter m_z^*, different from m^*, and/or a effective length different from L and consequently a parameter $\omega_{p,z}^2$ different from ω_p^2. It is easy to solve the anisotropic model and derive equivalent Eqs. (1) and (5). We did not succeed, however, with such an approach, to reduce the discrepancies of the model with respect to the experimental results, even by letting the parameters like θ or Ω varying noticeably. This is not unexpected because this additional correction to the model keeps the essential symmetry of the problem.

Our present understanding is that the asymmetry of the observed discrepancies reveals the existence of some interaction between the CR-like transition and the GaAs TO mode of the QW, as noticed experimentally.[14] Such an interaction is *a priori* quite surprising because it is known that the deformation potential of the conduction band with the TO mode is zero by symmetry in GaAs. Therefore, this will deserve some more elaborated theoretical treatment which remains to be done.

Finally, the proposed parabolic model is by construction symmetric in z, like the QWs to which the model has been applied: we found values fitted for $\hbar\Omega$ significantly lower than the intersubband splitting $\hbar\omega_{2,1}$ evaluated for a QW with infinite barriers (for instance in the present case $\hbar\Omega=65$ meV and $\hbar\omega_{2,1}\simeq92$ meV). One expects $\hbar\omega_{2,1}$ to be lower than the preceding estimate which is, assuming for m_z^*, the mean value of m^* used to fit the data in the PF configuration. One could improve the correspondence between energies by increasing $\omega_{p,z}^2$, using the anisotropic model described earlier, but the fit can only be done to a direct measurement of the corresponding intersubband absorption, which is very difficult for a simple QW. This, however, should help to evaluate the pertinence of the model.

Before concluding and, though it is not the purpose of the present paper, we would like to comment on the problem of the polaron coupling. Based on the Fröhlich interaction with a single electron this coupling is predicted to become resonant when the cyclotron energy coincides with the LO phonon energy.[19–21] This should manifest in the PF configuration as an anticrossing of the CR energies *around the LO energy* or, in other words, the CR transition energy should never cross that of the LO energy. It is clearly not apparent neither in the results of Fig. 1 nor on those obtained with carrier concentrations down to $6\times10^{11}\text{cm}^{-2}$.[14] We may argue that this carrier concentration is still too high and could screen the effect.[22] The problem on the experimental side is however not simple and requires to obtain data free of any dielectric artifacts in the range of LO energies. The data reported in Ref. 14 fulfill this requirement in GaAs. There are other systems based on GaInAs where such conditions are met, and it has been shown for instance in Ref. 23 that for samples with carrier concentration as low as $3\times10^{11}\text{cm}^{-2}$ no interaction of polaron character is seen around neither the GaAs-like nor the InAs-like LO energies. Therefore, the existence of polaronic effects on free carriers in real doped polar materials remains, in our opinion, not yet proved.

VII. CONCLUSION

Using a parabolic model to mimic the one-dimensional confinement of electron, we have derived all the components

of the dielectric tensor for the configuration when $\mathbf{k}//\mathbf{B}$, the plane of the 2D structure being tilted with respect to this direction. Using this model, we have derived the proper way to obtain a complete transmission response of any kind of multilayer structures containing conducting layers, in this tilted configuration. The comparison of the model with recent experimental data demonstrates that the model is globally satisfactory though its predictions deserve more experimental investigation.

ACKNOWLEDGMENTS

The GHMFL is "Laboratoire conventionné l'UJF et l'INPG de Grenoble." The work presented here has been supported in part by the European Commission through the Grant No. HPRI-CT-1999-00030. Y. B. acknowledges the support of Grant No. RFFI-03-02-16012.

APPENDIX

NP effects manifest themselves by different cyclotron frequencies for each couple of LL. Neglecting always the electron-electron interactions, one can treat the problem by assigning to each cyclotron frequency a family of carriers with a specific mass, relaxation time, and transition probability. This allows to include temperature effects eventually. The total electronic contribution to the dielectric constant is then simply obtained by adding the contribution of each family of carriers.

As an example, we consider NP effects only for the orbital part and neglect damping: for any value of the filling factor $\nu>2$ ($\nu=n_S/G_B$) which are not even, two different CR frequencies ω_{ca} and ω_{cb} have to be taken into account corresponding to two families of carriers with "effective" concentrations n_a, n_b, and masses m_a, m_b, respectively. The expressions for $\varepsilon_{xx}^{\mathrm{el}}$, in the PF configuration, with the present model and the one obtained from a quantum mechanical treatment read, respectively, as

$$\varepsilon_{xx}^{\mathrm{el}} = -4\pi e^2\left[\frac{n_a}{m_a(\omega^2-\omega_{ca}^2)}+\frac{n_b}{m_b(\omega^2-\omega_{cb}^2)}\right],$$

$$\varepsilon_{xx}^{\mathrm{el}} = -\frac{4\pi e^2 G_B}{L}\sum_{N=0}^{\infty}\sum_{\sigma}\frac{(f_{N,\sigma}-f_{N+1,\sigma})(N+1)}{m_N(\omega^2-\omega_{N+1,N,\sigma}^2)}, \quad \text{(A1)}$$

where $f_{N,\sigma}$ is the distribution function of carriers in the Nth LL with spin σ. In the limit of temperature going to zero, to make both expressions in Eq. (A1) compatible we are lead to make the following substitutions:

$$n_a \rightarrow G_B(2-\eta)N/L,$$

$$m_a \rightarrow m_N; \quad \omega_{ca} \rightarrow \omega_{N,N+1},$$

$$n_b \rightarrow G_B\eta(N+1)/L,$$

$$m_b \rightarrow m_{N+1}; \quad \omega_{cb} \rightarrow \omega_{N+1,N+2}, \quad \text{(A2)}$$

where η is the filling factor of the *higher* occupied LL including spin ($0<\eta<2$). This procedure can be easily extended to all components of the electronic part of the dielectric tensor. Therefore, the NP effects can be taken into account with this modification of the semiclassical model.

We further point out that the expression written in Eq. (A1) assumes for the probability of the transition the standard rules obtained in the one electron picture, though it is known that the CR transition has an excitonic character revealing the electron-electron interaction.[24] This excitonic nature may change these selection rules but since the overall model neglects the interactions between electrons, the procedure proposed in Eqs. (A1) and (A2) remains consistent.

[1] D. A. Dahl and L. J. Sham, Phys. Rev. B **16**, 651 (1977).
[2] C. Kallin and B. I. Halperin, Phys. Rev. B **30**, 5655 (1984).
[3] L. Wendler and R. Pechstedt, J. Phys.: Condens. Matter **2**, 8881 (1990).
[4] K. Karrai, S. Huant, G. Martinez, and L. C. Brunel, Solid State Commun. **66**, 355 (1988).
[5] D. W. Berreman, Phys. Rev. **130**, 2193 (1963).
[6] M. D. Sciacca, A. J. Mayur, Eunsoon Oh, A. K. Ramdas, S. Rodriguez, J. K. Furdyna, M. R. Melloch, C. P. Beetz, and W. S. Yoo, Phys. Rev. B **51**, 7744 (1995).
[7] See for instance G. Bastard, *Wave Mechanics Applied to Semiconductor Heterostructures* (Les Editions de la Physique, Paris, 1992).
[8] R. Merlin, Solid State Commun. **64**, 99 (1987).
[9] J. C. Maan, in *Two-Dimensional Systems, Heterostructures and Superlattices*, edited by G. Bauer, F. Kuchar, and H. Heinrich (Springer-Verlag, Berlin, 1984), Vol. 53, p. 183.
[10] H. C. Liu, and F. Capasso, in *Intersubband Transitions in Quantum Wells*, Semiconductors and Semimetals Vol. 62, edited by R. K. Willardson and E. R. Weber (Academic Press, New York, 2000).
[11] V. L. Ginzburg, *Propagation of Electromagnetic Waves in Plasma* (Gordon and Breach, New York, 1961).
[12] E. D. Palik and J. K. Furdyna, Rep. Prog. Phys. **33**, 1193 (1970).
[13] E. M. Lifshitz and L. P. Pitaevskii, *Physical Kinetics*, Landau and Lifshitz Course of Theoretical Physics Vol. 10, 2nd ed (Butterworth-Heinemann, Oxford, 1999).
[14] C. Faugeras, G. Martinez, A. Riedel, R. Rey, K. J. Friedland, and Yu. Bychkov, Phys. Rev. Lett. **92**, 107403 (2004).
[15] A. J. L. Poulter, J. Zeman, D. K. Maude, M. Potemski, G. Martinez, A. Riedel, R. Hey, and K. J. Friedland, Phys. Rev. Lett. **86**, 336 (2001).
[16] A. Pinczuk, J. M. Worlock, H. L. Störmer, R. Dingle, W. Wiegmann, and A. C. Gossard, Solid State Commun. **36**, 43 (1980).
[17] R. Kaplan, E. D. Palik, R. F. Wallis, S. Iwasa, E. Burstein, and Y. Sawada, Phys. Rev. Lett. **18**, 159 (1967).
[18] A. Mooradian and G. B. Wright, Phys. Rev. Lett. **16**, 999 (1966).
[19] S. Das Sarma, Phys. Rev. Lett. **52**, 859 (1984).

[20] F. M. Peeters and J. T. Devreese, Phys. Rev. B **31**, 3689 (1985).
[21] D. M. Larsen, Phys. Rev. B **30**, 4595 (1984).
[22] F. M. Peeters, X. G. Wu, J. T. Devreese, C. J. G. M. Langerak, J. Singleton, D. J. Barnes, and R. J. Nicholas, Phys. Rev. B **45**, 4296 (1992).
[23] R. J. Nicholas, L. C. Brunel, S. Huant, K. Karrai, J. C. Portal, M. A. Brummell, M. Razeghi, K. J. Cheng, and A. Y. Cho, Phys. Rev. Lett. **55**, 883 (1985).
[24] Yu. Bychkov and G. Martinez, Phys. Rev. B **66**, 193312 (2002).